

INTERACTION NOTES

Note 235

25 April 1975

DETERMINING THE NATURAL FREQUENCIES OF
SPHEROIDS VIA THE BOUNDARY-VALUE PROBLEM FORMULATION

R. J. Lytle
F. J. Deadrick

Lawrence Radiation Laboratory
Livermore, California

ABSTRACT

Equations by which one can determine the natural frequencies of prolate and oblate spheroids are derived using the boundary-value-problem approach. Both transverse magnetic and transverse electric excitations are considered. Numerical results are given for the natural frequencies of transverse-magnetic-excited prolate spheroids with various eccentricities, demonstrating natural mode dependence on eccentricity. Numerical difficulties, however, precluded obtaining natural frequencies for oblate spheroids, transverse-electric-excited prolate spheroids, and transverse-magnetic-excited prolate spheroids with sheaths.

TABLE OF CONTENTS

	Page
Abstract	1
Introduction	3
Background Information	4
Numerical Studies	10
Conclusions	12
References	19
Symbol Definitions	20

Introduction

Metallic structures excited by incident pulses radiate complex frequencies natural to the structures pulsed. These natural frequencies can be determined using integral-equation methods and boundary-value problem-formulation techniques, two classical analytical procedures. Integral equations, for example, have been used to find the natural frequencies of cylinders and the boundary-value problem formulation has been used in studying spheres. The integral-equation approach, however, can be applied to a wider variety of shapes than boundary-value problem formulation. Consequently, the majority of natural-frequency data available has been obtained using integral equations. Nonetheless, boundary-value-problem results are useful and are used in this study to examine the natural frequencies of prolate and oblate spheroids (ellipses rotated about their major and minor axes, respectively).

These spheroidal shapes are 2 of the 11 different orthogonal coordinate systems for which the scalar wave equation is separable. The other coordinate systems include: rectangular, circular cylinder, elliptic cylinder, parabolic cylinder, spherical, parabolic, conical, ellipsoidal, and paraboloidal. For these 11 systems, there are only 3 finite-sized, constant-coordinate surfaces¹: the sphere (occurring in the spherical and conical coordinate systems), the prolate spheroid (occurring in the prolate spheroidal system), and the oblate spheroid (occurring in the oblate spheroidal system). Our interest in prolate and oblate spheroids arises from the fact that many weapons problems (e.g., electromagnetic scattering from missiles and aircraft) concern finite-sized bodies.

While the natural frequencies of spheres have been tabulated extensively,^{2,3,4} the natural frequencies of prolate and oblate spheroids have not. Equations governing these frequencies can be determined, however, using a boundary-value problem-formulation technique analogous to that used in determining the natural frequencies of a sphere.

Background Information

It is assumed here that the reader is familiar with the spherical coordinate system, but unfamiliar with the prolate and oblate spheroidal coordinate systems⁵ (Figs. 1 and 2, respectively). Ellipses of various sizes are described in both the oblate and prolate systems by the parameter ξ . For the prolate system, $\xi \geq 1$, with $\xi = 1$ representing a needle and $\xi \rightarrow \infty$ representing a sphere. For the oblate system, $0 \leq \xi < \infty$, with $\xi = 0$ representing a disc and $\xi \rightarrow \infty$ representing a sphere. The parameter η describes a system of hyperbolas for both systems, and the variable ϕ is equivalent to the right circular cylindrical coordinate system variable ϕ . A degenerate case of both prolate and oblate spheroids is a sphere, occurring when the major and minor axes of the ellipse are equal.

Here, we are concerned with the source-free excitation of these finite sized bodies, with interest in both the transverse magnetic (TM) and transverse electric (TE) modes of oscillation. Because these natural modes have to satisfy the radiation condition at infinity, they must be outward-propagating modes. The radiation condition is automatically imposed on the natural-frequency model solutions for spheres and prolate and oblate spheroids.

When the sources of a field (thus, the field itself) do not vary with the coordinate ϕ , Maxwell's equations, expressed in the rotationally symmetric coordinate system (u, v, ϕ) , reduce to⁶

$$\frac{\partial}{\partial v} (h_\phi H_\phi) = j\omega\epsilon h_v h_\phi E_u, \quad (1)$$

$$\frac{\partial}{\partial u} (h_\phi H_\phi) = -j\omega\epsilon h_u h_\phi E_v, \quad (2)$$

$$\frac{\partial}{\partial u} (h_v E_v) - \frac{\partial}{\partial v} (h_u E_u) = -j\omega\mu h_u h_v H_\phi, \quad (3)$$

$$\frac{\partial}{\partial v} (h_\phi E_\phi) = -j\omega\mu h_v h_\phi H_u, \quad (4)$$

$$\frac{\partial}{\partial u} (h_\phi E_\phi) = +j\omega\mu h_u h_\phi H_v, \quad (5)$$

$$\frac{\partial}{\partial u} (h_v H_v) - \frac{\partial}{\partial v} (h_u H_u) = +j\omega\epsilon h_u h_v H_\phi. \quad (6)$$

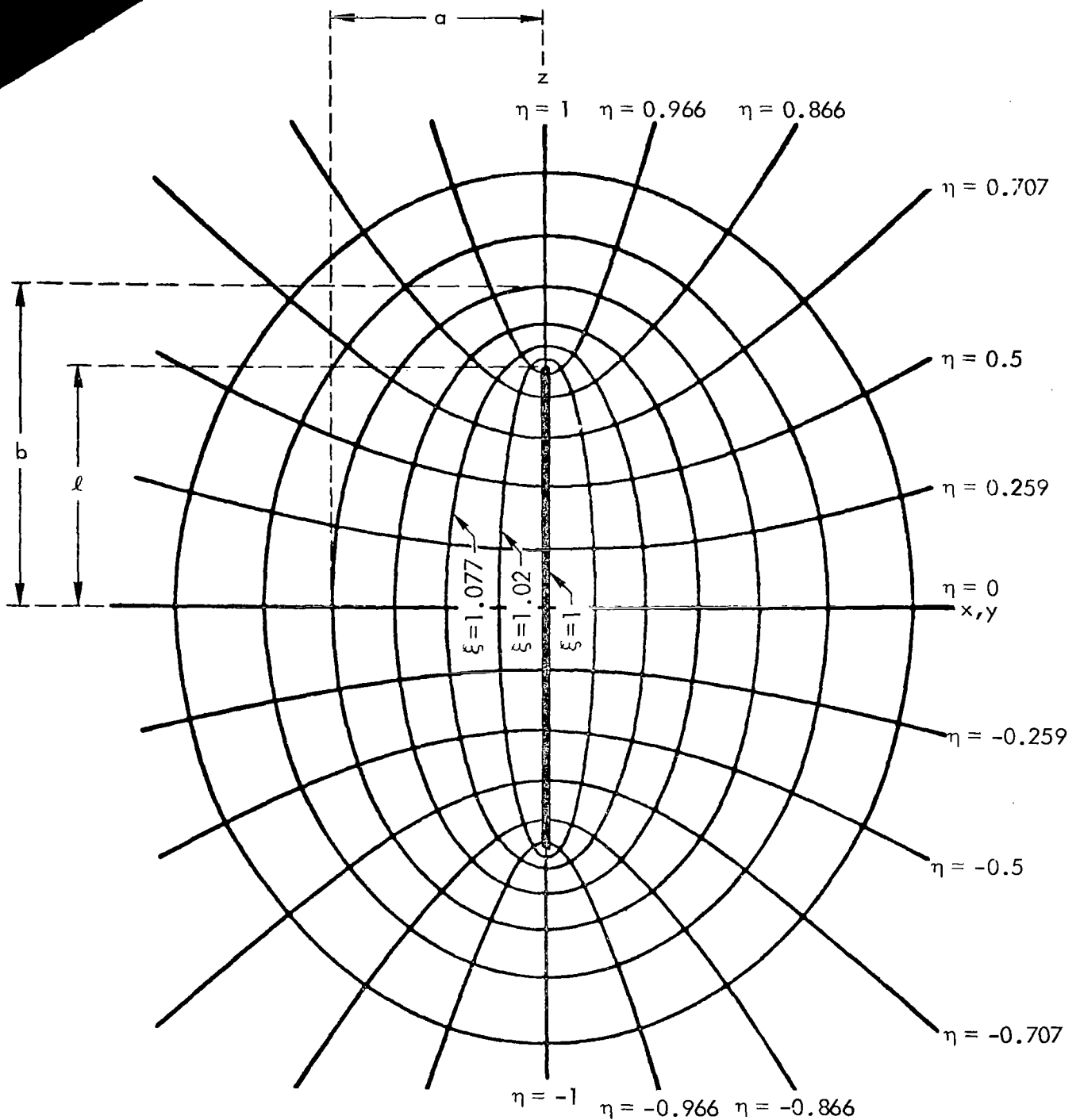


Fig. 1. The prolate spheroidal coordinate system (l = semifocal length, a = semiminor axis, b = semimajor axis).

The quantities h_u, h_v, h_ϕ are scale factors for the coordinate system, and (E_u, E_v, E_ϕ) and (H_u, H_v, H_ϕ) are, respectively, the orthogonal components of the electric and magnetic field intensities in the (u, v, ϕ) coordinate system. The $u, v, \phi, h_u, h_v, h_\phi$ variables are identified in Table 1 in terms of the different coordinate-system variables.

Combining Eqs. (1) through (3) or (4) through (6) and defining $A = h_\phi H_\phi$ or $A = h_\phi E_\phi$ results in

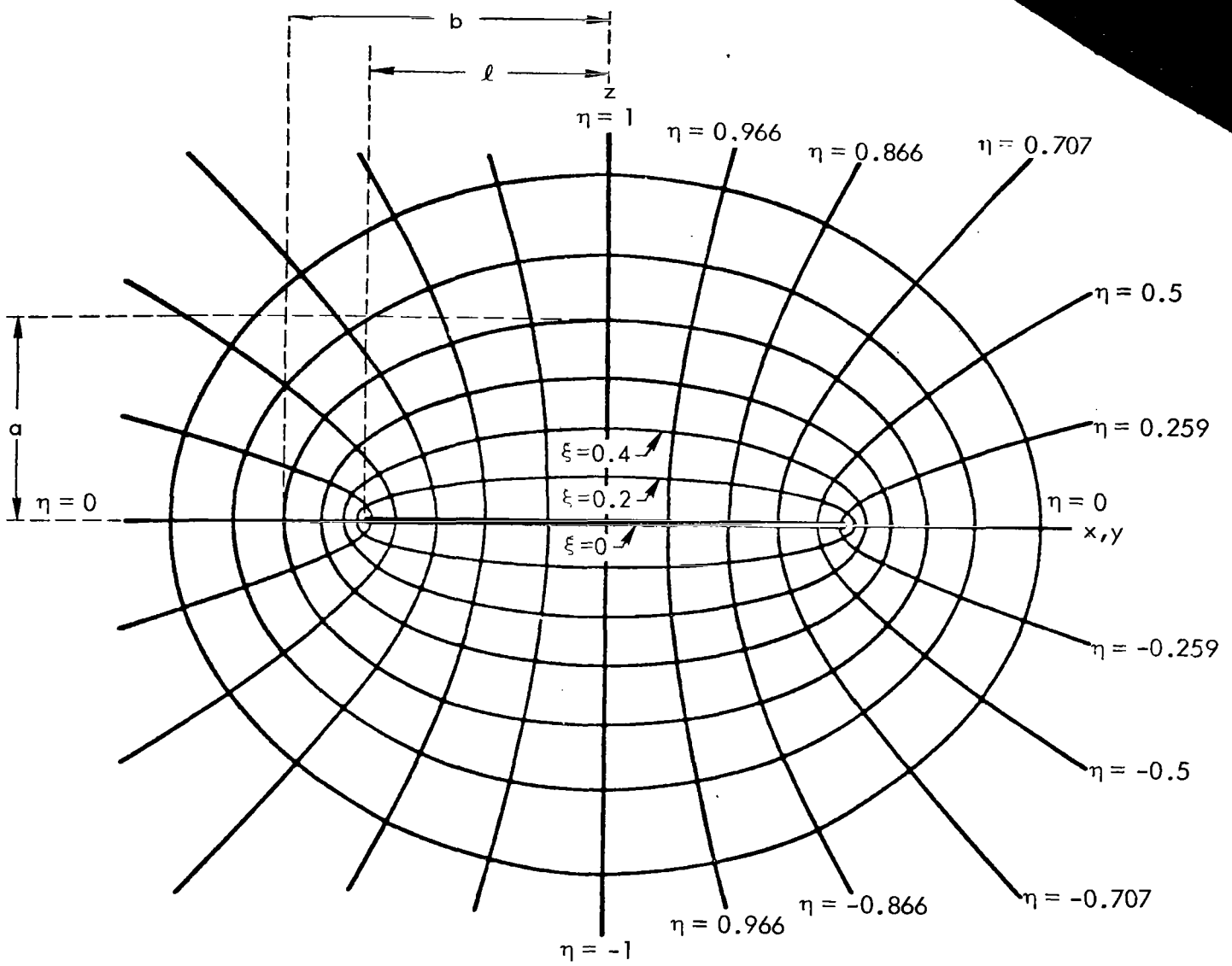


Fig. 2. The oblate spheroidal coordinate system (l = semifocal length, a = semiminor axis, b = semimajor axis).

$$\frac{\partial}{\partial u} \left(\frac{h_v}{h_\phi h_u} \frac{\partial A}{\partial u} \right) + \frac{\partial}{\partial v} \left(\frac{h_u}{h_\phi h_v} \frac{\partial A}{\partial v} \right) + \omega^2 \mu \epsilon \frac{h_u h_v}{h_\phi} A = 0 . \quad (7)$$

The coordinates u and v are separated into

$$\frac{h_v h_\phi}{h_u} \frac{d^2 U}{du^2} + [f_1(u) \omega^2 \mu \epsilon - s] U = 0 , \quad (8)$$

$$\frac{h_u h_\phi}{h_v} \frac{d^2 V}{dv^2} + [f_2(v) \omega^2 \mu \epsilon + s] V = 0 , \quad (9)$$

where s is the separation constant and the quantities $f_1(u)$, $f_2(v)$, $h_v h_\phi / h_u$, and $h_u h_\phi / h_v$ are given in Table 2. Also given in Table 2 are the solutions of Eqs. (8) and (9) in the respective coordinate systems. 6

Table 1. Definitions of orthogonal variables and scale factors.

Spherical	Prolate spheroidal	Oblate spheroidal
$u = r$	$u = \xi$	$u = \xi$
$v = -\cos \theta$	$v = \eta = \cos \theta$	$v = \eta = \cos \theta$
$\phi = \phi$	$\phi = \phi$	$\phi = \phi$
$h_u = 1$	$h_u = \ell \sqrt{\frac{\xi^2 - \eta^2}{\xi^2 - 1}}$	$h_u = \ell \sqrt{\frac{\xi^2 + \eta^2}{\xi^2 + 1}}$
$h_v = \frac{r}{\sin \theta}$	$h_v = \ell \sqrt{\frac{\xi^2 - \eta^2}{1 - \xi^2}}$	$h_v = \ell \sqrt{\frac{\xi^2 + \eta^2}{1 - \xi^2}}$
$h_\phi = r \sin \theta$	$h_\phi = \ell \sqrt{(\xi^2 - 1)(1 - \eta^2)}$	$h_\phi = \ell \sqrt{(\xi^2 + 1)(1 - \eta^2)}$

Table 2. Useful relationships for use in Eqs. (8) and (9) and the characteristic solutions of these equations.

Spherical	Prolate spheroidal	Oblate spheroidal
$f_1(u) = r^2$	$f_1(u) = \ell^3 \xi^2$	$f_1(u) = \ell^3 \xi^2$
$f_2(v) = 0$	$f_2(v) = -\ell^3 \eta^2$	$f_2(v) = \ell^3 \eta^2$
$\frac{h_v h_\phi}{h_u} = r^2$	$\frac{h_v h_\phi}{h_u} = \ell(\xi^2 - 1)$	$\frac{h_v h_\phi}{h_u} = \ell(\xi^2 + 1)$
$\frac{h_u h_\phi}{h_v} = \sin^2 \theta$	$\frac{h_u h_\phi}{h_v} = \ell(1 - \eta^2)$	$\frac{h_u h_\phi}{h_v} = \ell(1 - \eta^2)$
$U(u) = rz_n^{(i)}(kr)$	$U(u) = \sqrt{\xi^2 - 1} R_{\ln}^{(i)}(c, \xi)$	$U(u) = \sqrt{\xi^2 + 1} R_{\ln}^{(i)}(-ic, i\xi)$
$V(v) = P_n^m(-\cos \theta)$	$V(v) = \sqrt{1 - \eta^2} S_{\ln}(c, \eta)$	$V(v) = \sqrt{1 - \eta^2} S_{\ln}(-ic, \eta)$

NOTE: $c = \omega \sqrt{\mu \epsilon} \ell$.

The constant coordinate variable specifying a sphere is $u=u_0=r_0$, that specifying a prolate spheroid is $u=u_0=\xi_0$, and that specifying an oblate spheroid is $u=u_0=\xi_0$. For metallic spheres and spheroids, the tangential electric fields on the metallic surface $u=\text{constant}=u_0$ are zero. This constraint specifies the natural frequencies, as shown in the following paragraph.

For TM fields (E_u, E_v, H_ϕ), the surface tangential electric field is E_v . Using Eq. (2) and applying the boundary condition at the surface u_0 ,

$$E_v = - \frac{1}{j\omega\epsilon h_u h_\phi} \frac{\partial}{\partial u} (h_\phi H_\phi) \Big|_{u=u_0} = 0 .$$

The quantity $h_\phi H_\phi = A$ satisfies Eq. (7), with solutions given in Table 2. Using Eq. (10) and the results in Tables 1 and 2, we can show that the source-free TM excitation of a metallic sphere satisfies

$$\frac{\partial}{\partial r} \left[r h_n^{(2)}(kr) \right] \Big|_{r=r_0} = 0 , \quad (11)$$

the source-free TM excitation of a metallic prolate spheroid satisfies

$$\frac{\partial}{\partial \xi} \left[\sqrt{\xi^2 - 1} R_{\ln}^{(4)}(c, \xi) \right] \Big|_{\xi=\xi_0} = 0 , \quad (12)$$

and the source-free TM excitation of a metallic oblate spheroid satisfies

$$\frac{\partial}{\partial \xi} \left[\sqrt{\xi^2 + 1} R_{\ln}^{(4)}(-ic, i\xi) \right] \Big|_{\xi=\xi_0} = 0 . \quad (13)$$

In Eqs. (11) through (13), the radiation condition on the source-free solutions has been imposed on the appropriate $U(u)$ functional behavior described in Table 2 [i.e., $z_n^{(m)}(kr) = h_n^{(2)}(kr)$, $R_{\ln}^{(m)}(c, \xi) = R_{\ln}^{(4)}(c, \xi)$, and $R_{\ln}^{(m)}(-ic, i\xi) = R_{\ln}^{(4)}(-ic, i\xi)$].

Equation (11) is the well-known condition for determining the TM natural frequencies of a metallic sphere.^{2,3} Equations (12) and (13) are the not-so-well-known conditions for determining the TM natural frequencies of metallic prolate and oblate spheroids, respectively. These results can be inferred, however, from previous work pertaining to metallic prolate⁷⁻⁹ and oblate¹⁰⁻¹² spheroids with TM excitation.

For TE fields (H_u, H_v, E_ϕ), the surface tangential electric field is E_ϕ . Using Eqs. (4) through (7), Tables 1 and 2, and the condition $E_\phi = 0$ at $u=u_0$,

$$E_\phi = \frac{1}{h_\phi} U(u_0) V(v) = 0 . \quad (14)$$

Thus, from Table 2, it is seen that the source-free TE excitation of a metallic sphere satisfies

$$h_n^{(2)}(kr_0) = 0 , \quad (15)$$

the source-free TE excitation of a metallic prolate spheroid satisfies

$$R_{\ln}^{(4)}(c, \xi_0) = 0 , \quad (16)$$

ice-free TE excitation of a metallic oblate spheroid satisfies

$$R_{1n}^{(4)}(-ic, i\xi_0) = 0 . \quad (17)$$

Here, Eq. (15) is the well-known condition for determining the TE natural frequencies of a metallic sphere,^{2,3} and Eqs. (16) and (17) are the not-so-well-known conditions for determining the TE natural frequencies of metallic prolate and oblate spheroids, respectively. These results also can be inferred from earlier research on metallic prolate⁹ and oblate¹⁰⁻¹² spheroids with TE excitation.

The prolate spheroid with TM excitation has been studied previously by Marin,¹³ who sampled the field at 32 locations and used an integral-equation formulation to determine natural frequencies. In this study, we compare the exact boundary value with approximate integral-equation results for a prolate spheroid to illustrate their close correlation.

Also of interest is the effect a sheath surrounding a metallic object has on the natural frequencies of the object. This effect can be determined for a sphere (for TM and TE excitations) and for a prolate spheroid¹⁴ (for a TM excitation). The governing equation for a TM-excited metallic spheroid (described by $\xi = \xi_{in}$) surrounded by a confocal sheath (between the surfaces $\xi = \xi_{in}$ and $\xi = \xi_{out}$) is that the determinant of A is zero, where

$$A = \begin{pmatrix} P_1 & P_2 & Q_1 \\ P_3 & P_4 & 0 \\ R_1 & R_2 & S_1 \end{pmatrix} \quad (18)$$

with $P_1, P_2, P_3, P_4, R_1,$ and R_2 being diagonal matrices in which the m th elements (with m odd and $\ell = \frac{m+1}{2}$) are

$$(P_1)_{\ell\ell} = R_{1m}^{(1)}(c_{in}, \xi_{out}) , \quad (19)$$

$$(P_2)_{\ell\ell} = R_{1m}^{(2)}(c_{in}, \xi_{out}) , \quad (20)$$

$$(P_3)_{\ell\ell} = \frac{\partial}{\partial \xi} \left[\sqrt{\xi^2 - 1} R_{1m}^{(1)}(c_{in}, \xi) \right] \Big|_{\xi=\xi_{in}} , \quad (21)$$

$$(P_4)_{\ell\ell} = \frac{\partial}{\partial \xi} \left[\sqrt{\xi^2 - 1} R_{1m}^{(2)}(c_{in}, \xi) \right] \Big|_{\xi=\xi_{in}} , \quad (22)$$

$$(R_1)_{\ell\ell} = \frac{\partial}{\partial \xi} \left[\sqrt{\xi^2 - 1} R_{1m}^{(1)}(c_{in}, \xi) \right] \Big|_{\xi=\xi_{out}} , \quad (23)$$

$$(R_2)_{\ell\ell} = \frac{\partial}{\partial \xi} \left[\sqrt{\xi^2 - 1} R_{1m}^{(2)}(c_{in}, \xi) \right] \Big|_{\xi=\xi_{out}} . \quad (24)$$

Matrices Q_1 and S_1 are general matrices with elements of (with m and n odd and $l = \frac{m+1}{2}$ and $k = \frac{n+1}{2}$)

$$(Q_1)_{lk} = -N_{mn} R_{ln}^{(4)}(c_{out}, \xi_{out}), \quad (25)$$

$$(S_1)_{lk} = -\frac{\epsilon_{in}}{\epsilon_{out}} N_{mn} \frac{\partial}{\partial \xi} \left[\sqrt{\xi^2 - 1} R_{ln}^{(4)}(c_{in}, \xi) \right] \Big|_{\xi=\xi_{out}}, \quad (26)$$

where

$$N_{mn} = \int_{-1}^{+1} S_{ln}(c_{out}, \eta) S_{lm}(c_{in}, \eta) d\eta. \quad (27)$$

Note that, although matrix A is infinite, it can be truncated to a large, but finite, size. One can then vary c to approximate natural frequencies for various combinations of ϵ_{in} , ϵ_{out} , l , ξ_{in} , and ξ_{out} .

Numerical Studies

It is recognized, of course, that degenerate cases of both prolate and oblate spheroids can be spheres. A second degenerate case of a prolate spheroid is a needle, and a second degenerate case of an oblate spheroid is a disc. In this study using the boundary-value-problem approach, we are interested in the behavior of natural frequencies for spheroids between these two extremes. As noted earlier, others have presented boundary-value-problem results for spheres,²⁻⁴ and approximate integral-equation results for prolate spheroids.¹³ The numerical studies reported here are meant to complement this previous work.

The numerical approach used in this analysis was to evaluate the spheroidal functions¹⁵ of complex argument c ($c = \omega\sqrt{\mu\epsilon}l$) for a number of c values and to use optimization procedures to determine those values of c that best meet the prescribed conditions. This approach has been used previously for the sphere.³

Numerical results for the natural frequencies of a TM-excited, perfectly conducting prolate spheroid in an infinite medium are shown in Fig. 3. The results shown are for the first layer of poles. Several shape factors are presented (spheroid major-to-minor axis ratios b/a of 1, 5, 10, and 100) to illustrate the dependence of the natural frequencies on object shape. As the eccentricity of the spheroids is enhanced ($\frac{b}{a} \rightarrow \infty$), the poles approach the asymptotic limit of poles for a thin cylinder,¹⁶ a result demonstrated in previous studies.^{4,13}

The boundary-value-problem results shown in Fig. 3 were compared with the integral-equation results obtained by Marin,¹³ and the agreement was good. This can be seen by comparing Marin's integral-equation results with the boundary-value-problem results for

first layer of poles (see Tables 3 and 4). Agreement is quite good, considering the different approaches used in determining the natural frequencies.

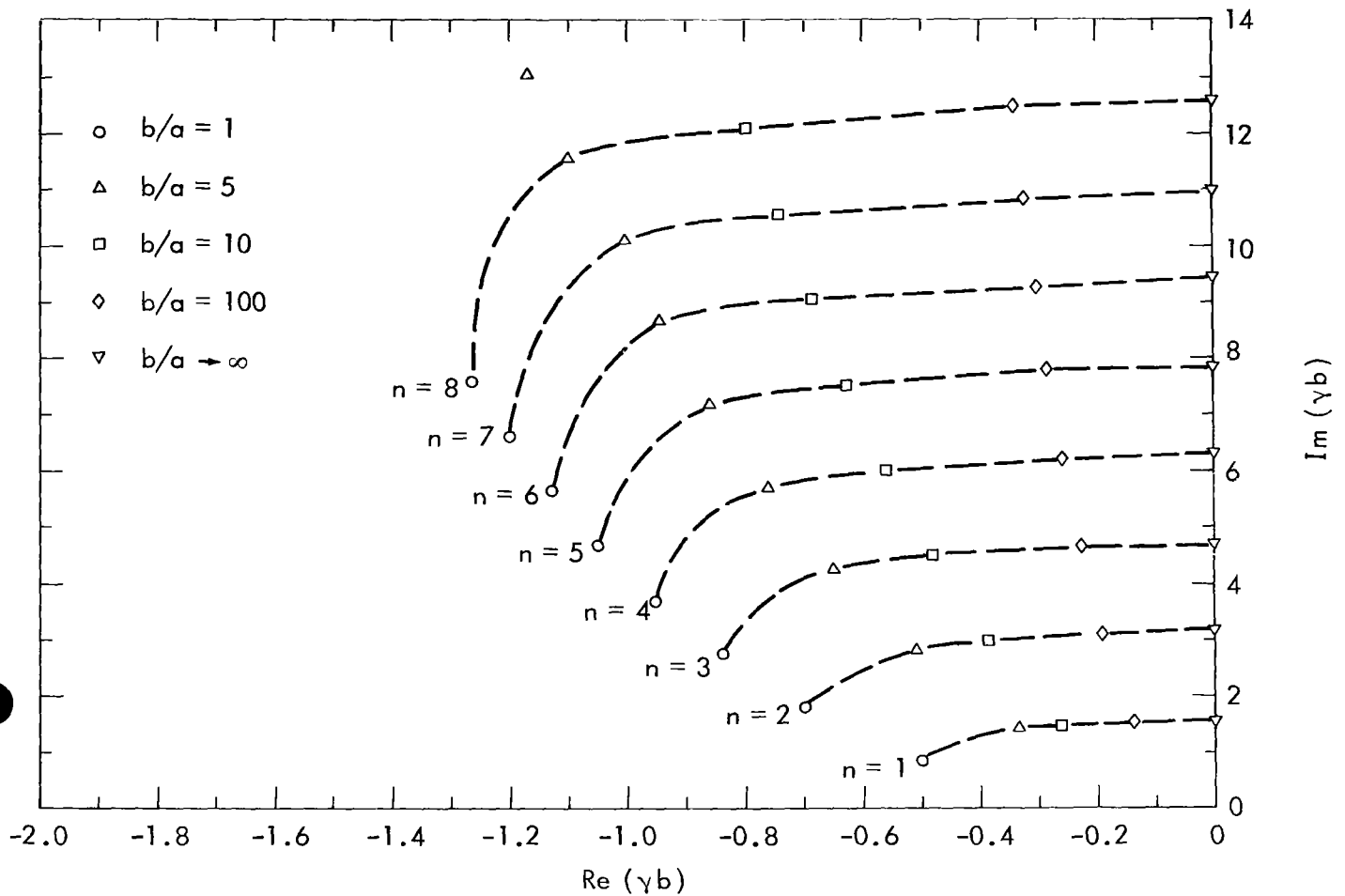


Fig. 3. Locus of natural frequencies for TM-excited prolate spheroids with various eccentricities. (Note: $\gamma = \omega\sqrt{\mu\epsilon}$, $b = \ell\xi_0$.)

Table 3. Integral-equation versus boundary-value-problem results for γb with a major-to-minor axis of 10:1.

Pole number	Integral equation	Boundary-value problem
1	-0.265 + i 1.458	-0.263 + i 1.453
2	-0.391 + i 2.955	-0.391 + i 2.955
3	-0.497 + i 4.510	-0.485 + i 4.467
4	-0.582 + i 6.051	-0.562 + i 5.985
5	-0.658 + i 7.598	-0.630 + i 7.506
6	-0.727 + i 9.149	-0.690 + i 9.030
7	-0.793 + i 10.703	-0.744 + i 10.56
8	-0.855 + i 12.260	-0.795 + i 12.08

Table 4. Integral-equation versus boundary-value-problem results for γb with a major to-minor axis of 5:1.

Pole number	Integral equation	Boundary-value problem
1	-0.336 + i 1.374	-0.335 + i 1.402
2	-0.516 + i 2.817	-0.512 + i 2.807
3	-0.655 + i 4.277	-0.648 + i 4.257
4	-0.773 + i 5.745	-0.761 + i 5.713
5	-0.876 + i 7.220	-0.860 + i 7.175
6	-0.970 + i 8.698	-0.949 + i 8.639
7	-1.057 + i 10.180	-1.03 + i 10.11
8	-1.138 + i 11.666	-1.10 + i 11.57

An interesting sidelight was to compute the angle functions $S_{ln}(c, \eta)$ for the values of c corresponding to natural frequencies. (The functions were normalized using Flammer's⁵ normalization procedure.) This was done for various eccentricities as there was some speculation¹⁷ concerning the natural mode behavior for spheroids of various eccentricities. As shown in Figs. 4 through 9, the angle functions $S_{ln}(c, \eta)$ are predominately real, but have a finite imaginary component. This is consistent with Marin's observations.¹³ Also, as eccentricity increases, the variation of the angle functions $S_{ln}(c, \eta)$ departs from Legendre function behavior and approaches that of a pure, real angle function of $\sin \frac{m\pi\eta}{2}$ and $\cos \frac{m\pi\eta}{2}$.

Unfortunately, numerical difficulties were encountered in solving the oblate-spheroidal and the TE-excited prolate-spheroidal problems. A few poles could be found, but the overall layer structure could not be defined. Due to the large number of numerical problems encountered, this effort was terminated.

A number of attempts were made to attain reasonable answers to the problem of a TM-excited prolate spheroid with a sheath. However, after much effort with no discernible progress, this effort was abandoned. Several root-finding procedures^{18,19} were tried, but reasonable results were precluded by the numerical noise generated in formulating the spheroidal functions, the errors contributed by using a truncated matrix to approximate the infinite matrix, and the sensitivity of the root-finding procedures to noise.

Conclusions

This study demonstrates that the analytical expressions by which one can determine the TM and TE natural frequencies of prolate and oblate spheroids can be derived using the boundary-value-problem approach. Also, numerical results for the natural frequencies of a TM-excited, prolate-spheroidal, metallic object can be evaluated using

is technique. Moreover, these boundary-value-problem results compare favorably with previously obtained results based on integral equation formulation. Numerical difficulties, however, prevented obtaining natural frequencies for oblate spheroids, a TE-excited prolate spheroid, and a TM-excited prolate spheroid with a sheath.

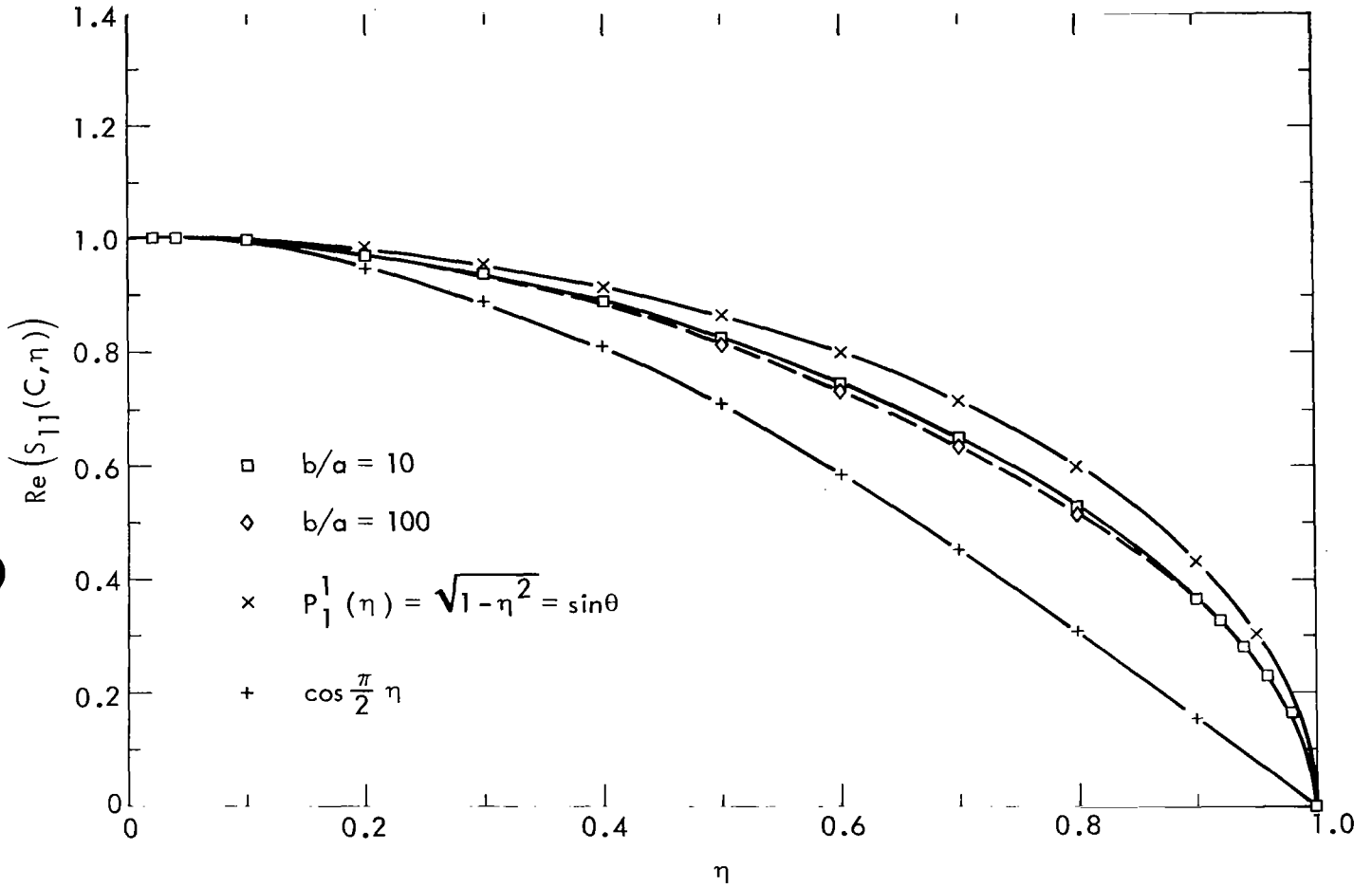


Fig. 4. Natural frequency behavior of $S_{11}(c, \eta)$ is predominantly real and appears to pass from Legendre function behavior (for $b/a = 1$) to $\cos \frac{\pi}{2} \eta$ behavior as eccentricity increases. (Note: $z = \ell \xi_0 \eta$.)

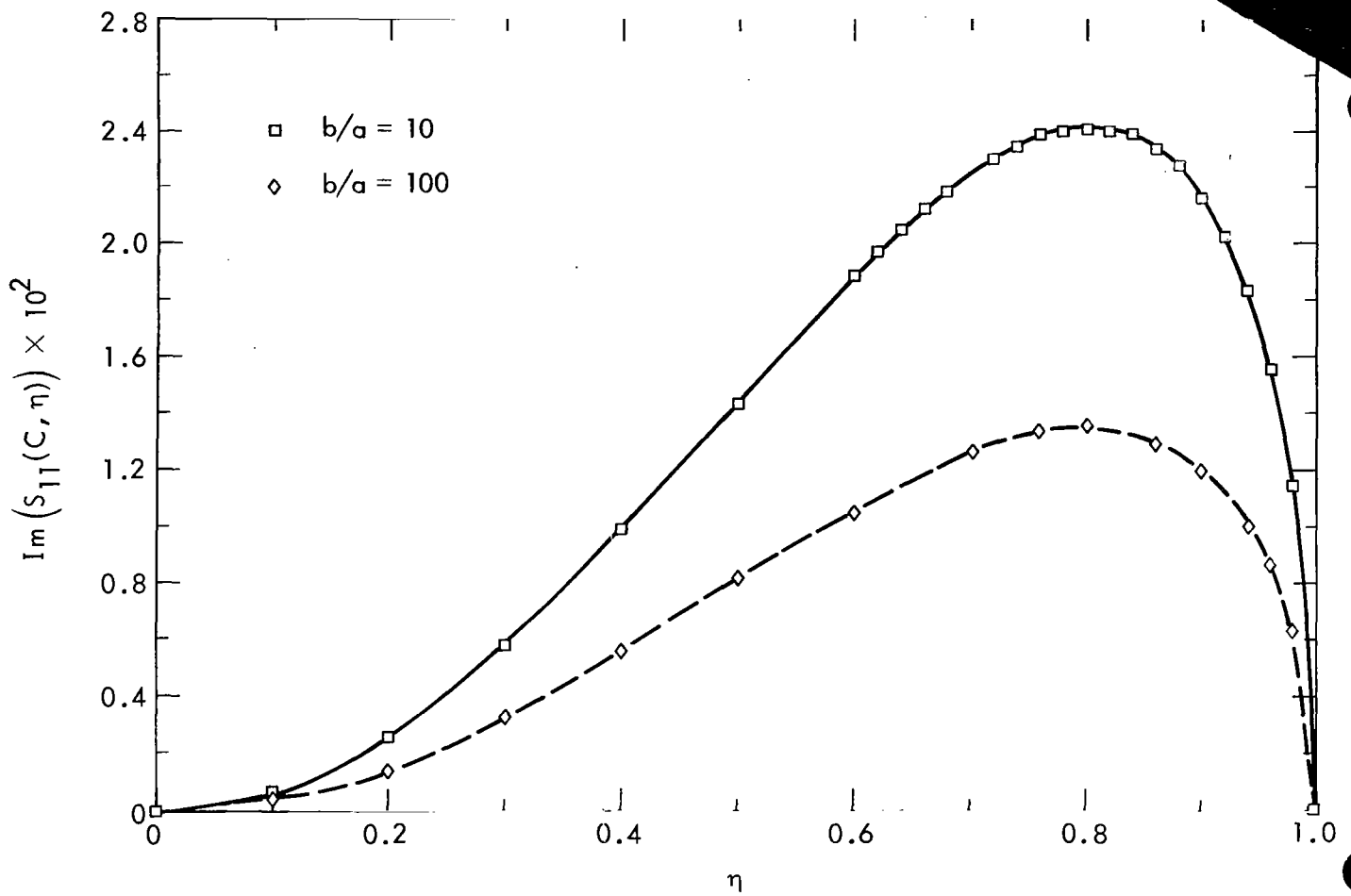


Fig. 5. Natural frequency behavior of $S_{11}(c, \eta)$ is predominantly real and appears to pass from Legendre function behavior (for $b/a = 1$) to $\cos \frac{\pi}{2} \eta$ behavior as eccentricity increases.

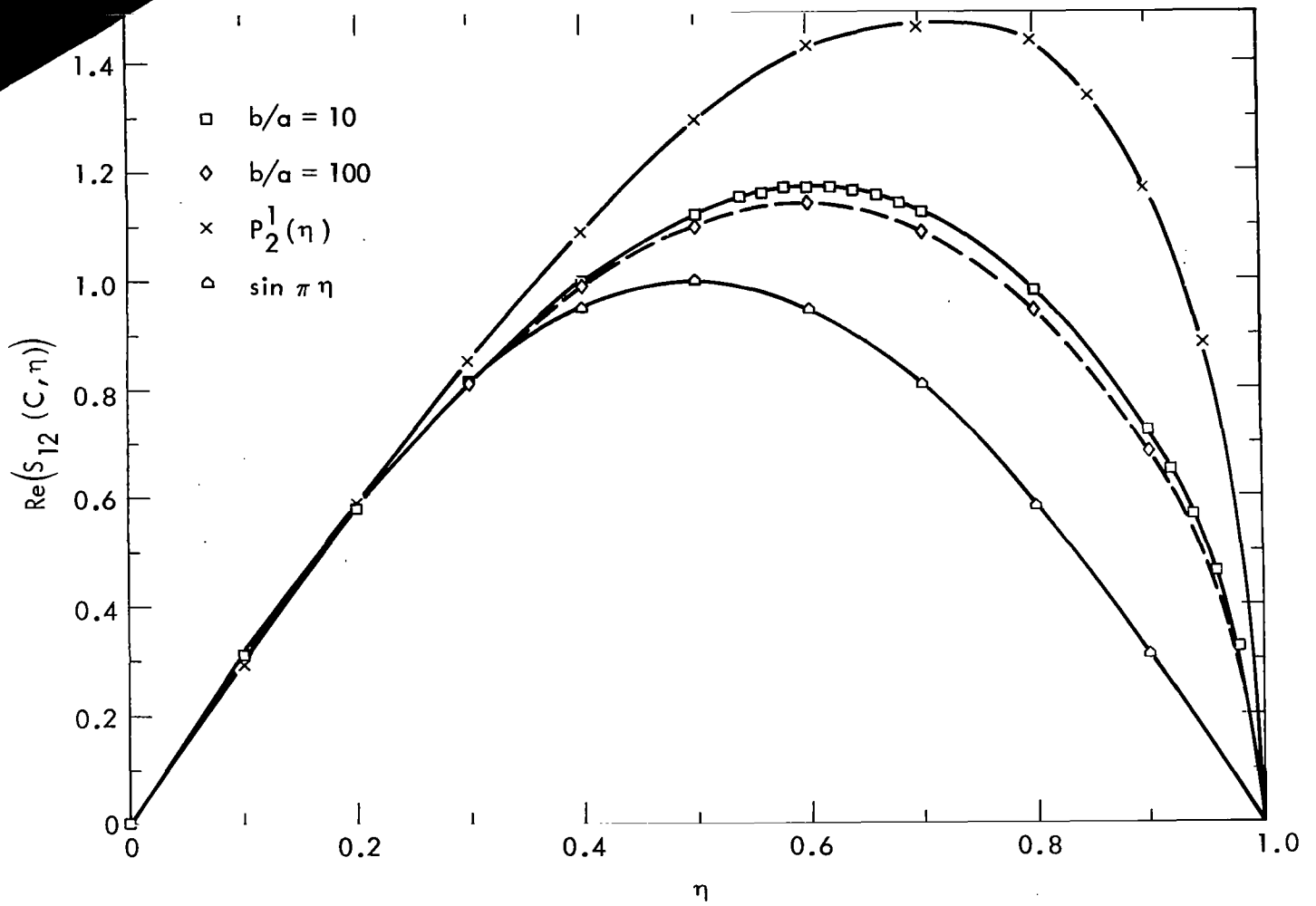


Fig. 6. Natural frequency behavior of $\text{Re}(S_{12}(c, \eta))$ is predominantly real and appears to pass from Legendre function behavior (for $b/a = 1$) to $\sin \pi \eta$ behavior as eccentricity increases.

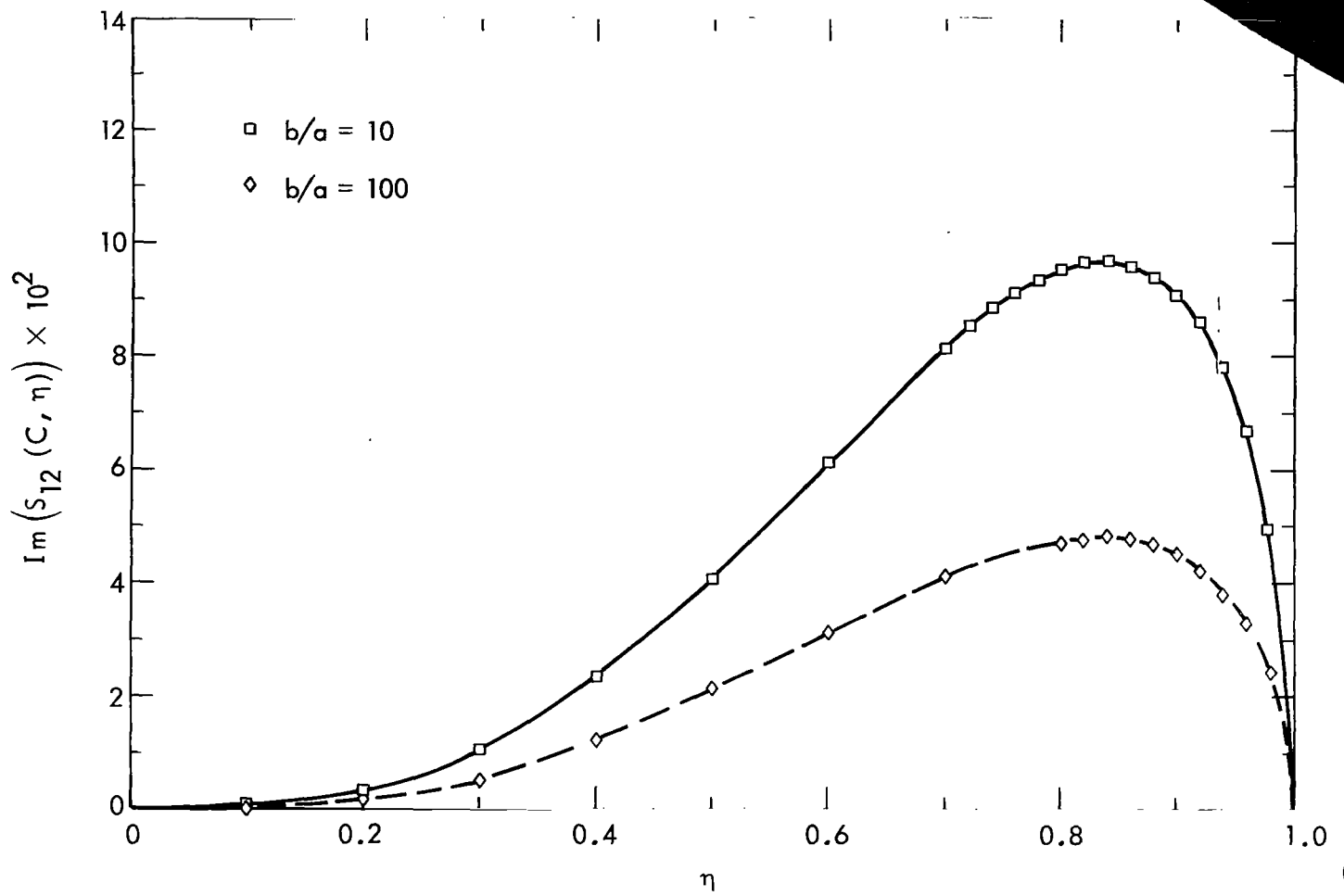


Fig. 7. Natural frequency behavior of $\text{Re}(S_{12}(c, \eta))$ is predominantly real and appears to pass from Legendre function behavior (for $b/a = 1$) to $\sin \pi \eta$ behavior as eccentricity increases.

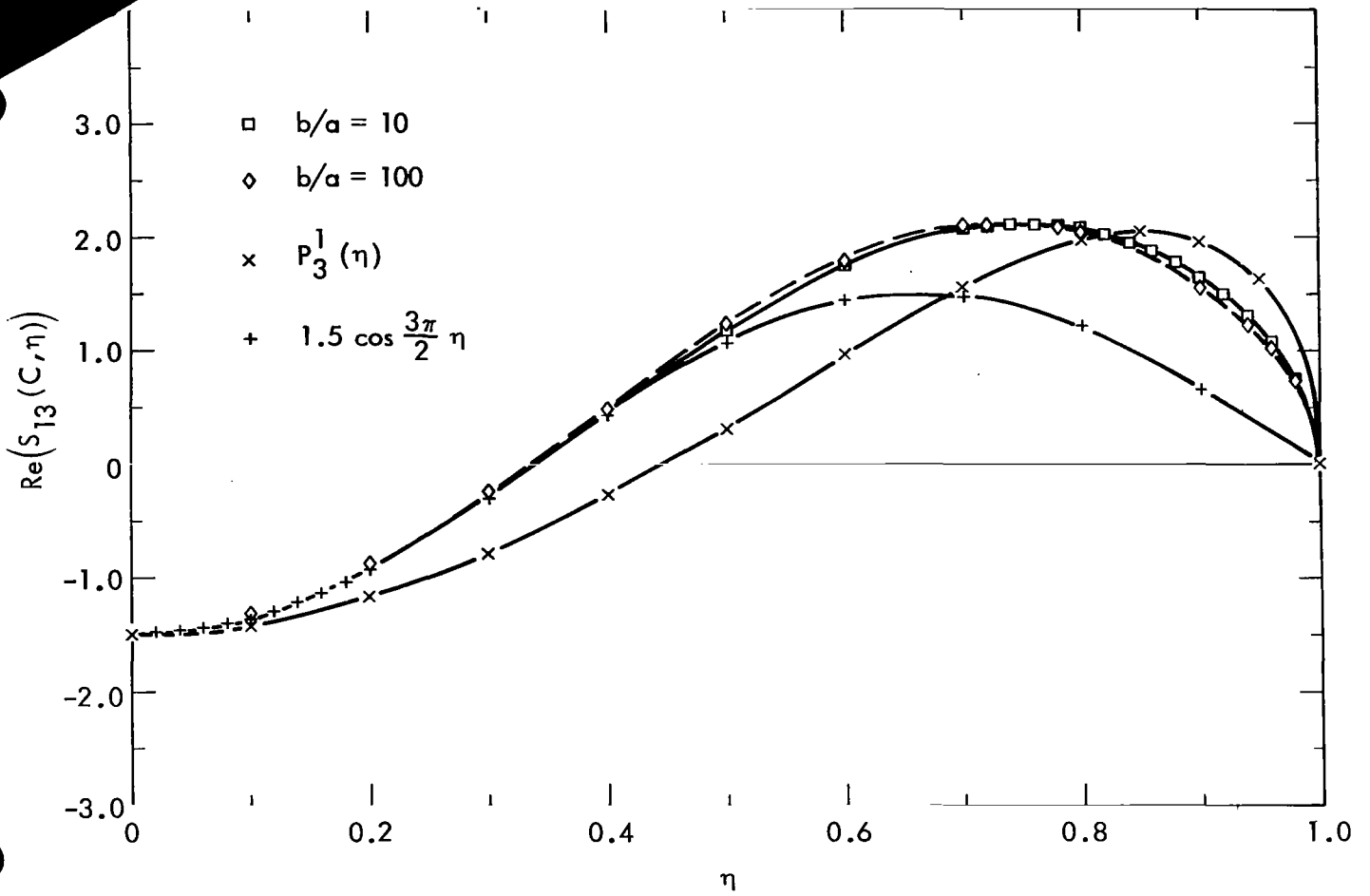


Fig. 8. Natural frequency behavior of $S_{13}(c, \eta)$ is predominantly real and appears to pass from Legendre function behavior (for $b/a = 1$) to $\cos \frac{3\pi}{2} \eta$ behavior as eccentricity increases.

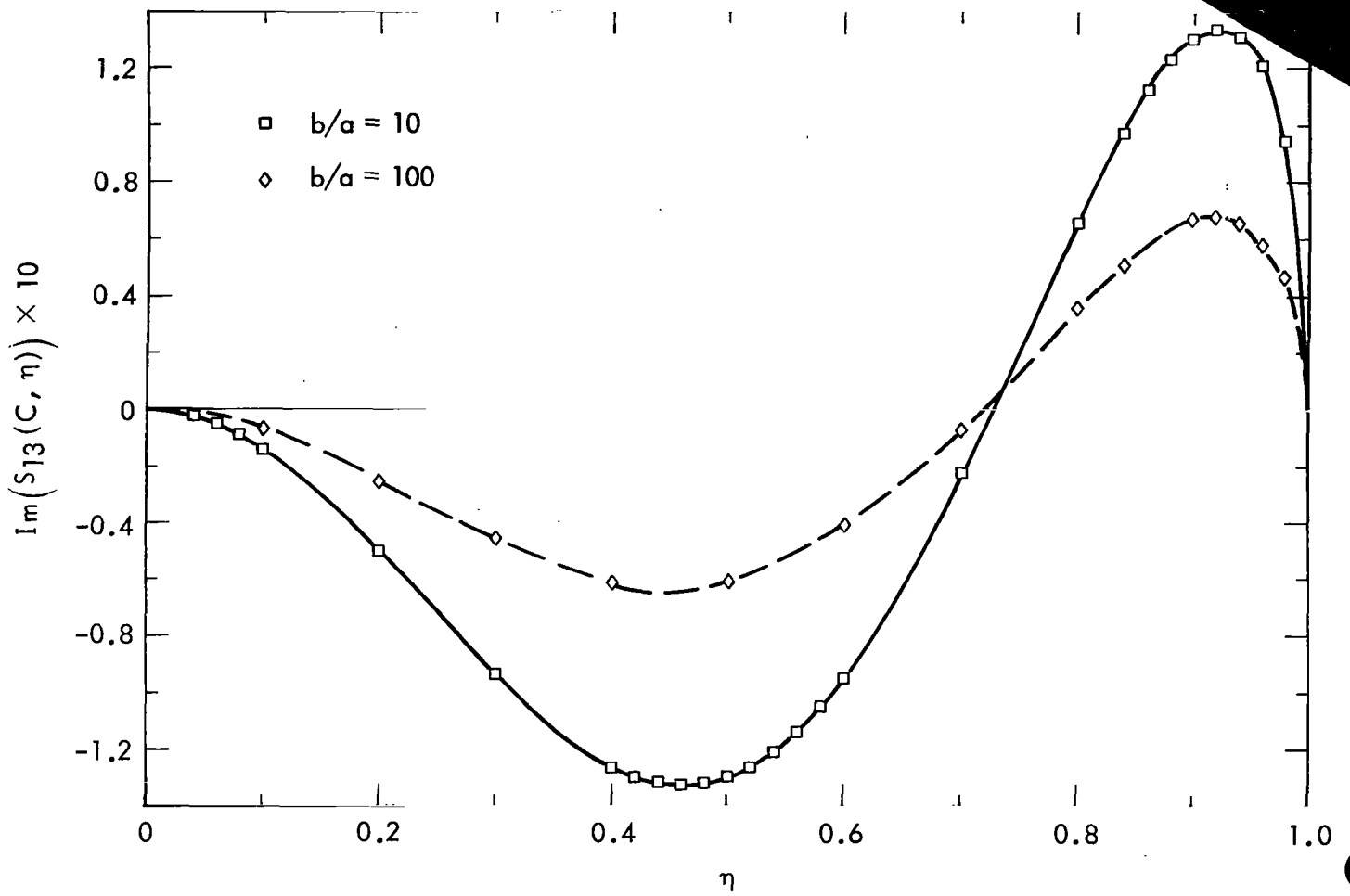


Fig. 9. Natural frequency behavior of $S_{13}(c, \eta)$ is predominantly real and appears to pass from Legendre function behavior (for $b/a = 1$) to $\cos \frac{3\pi}{2} \eta$ behavior as eccentricity increases.

References

1. P. Moon and D. E. Spencer, Field Theory Handbook (Springer-Verlag, Berlin, 1961).
2. C. E. Baum, On the Singularity Expansion Method for the Solution of Electromagnetic Interaction Problems, Interaction Note 88 (1971).
3. J. P. Martinez, J. L. Pine, and R. M. Tesch, Numerical Results of the Singularity Expansion Method as Applied to Plane Wave Incident on a Perfectly Conducting Sphere, Air Force Weapons Laboratory, Albuquerque, NM, Interaction Note 112 (1972).
4. F. M. Tesche, On the Singularity Expansion Method As Applied to Electromagnetic Scattering By Thin Wires, Air Force Weapons Laboratory, Albuquerque, NM, Interaction Note 102 (1972), see also IEEE Trans. on Antennas and Propagation AP-21, 53-62 (1973).
5. C. Flammer, Spheroidal Wave Functions (Stanford Univ. Press, Palo Alto, CA, 1975).
6. W. L. Weeks, Electromagnetic Theory for Engineering Applications (John Wiley & Sons, Inc., New York, 1964).
7. J. R. Wait, Radio Sci. 1, 475 (1966).
8. C. D. Taylor, Radio Sci. 2, 351 (1967).
9. J. R. Wait, "Electromagnetic Radiation From Spheroidal Structures," Antenna Theory, Part I, R. E. Collin and F. J. Zucker, Eds. (McGraw-Hill Book Company, New York, 1969), Chpt. 13.
10. C. Flammer, J. Appl. Phys. 24, 1218 (1953).
11. J. Meixner, Ann. Physik. Lpz. 12 (Ser. 6), 227-236 (1953).
12. C. Flammer, Radiation from Electric and Magnetic Dipoles in the Presence of a Conducting Circular Disk, Stanford Research Institute, Tech. Rept. 49, Menlo Park, CA (1955).
13. L. Marin, Natural-Made Representation of Transient Scattering from Rotationally Symmetric, Perfectly Conducting Bodies and Numerical Results for a Prolate Spheroid, Air Force Weapons Laboratory, Albuquerque, NM, Interaction Note 119 (1972).
14. R. J. Lytle and F. V. Schultz, IEEE Trans. on Antennas and Propagation AP-17 (No. 4), 496-506 (1969).
15. R. J. Lytle and F. J. Deadrick, Prolate and Oblate Spheroidal Wave Functions of Complex Argument, Air Force Weapons Laboratory, Albuquerque, NM, Mathematics Note 32 (1973).
16. S. W. Lee and B. Leung, The Natural Resonance Frequency of a Thin Cylinder and Its Application to EMP Studies, Air Force Weapons Laboratory, Albuquerque, NM, Interaction Note 96 (1972).
17. C. E. Baum, Air Force Weapons Laboratory, private communication (Dec. 10, 1974).
18. W. I. Zangwill, Computer Journal 10, 293-296 (1967).
19. S. I. Gass, Linear Programming (McGraw-Hill, New York, 1969).

Symbol Definitions

j	$\sqrt{-1}$
ω	Angular frequency
ϵ	Permittivity of the medium
μ	Permeability of the medium
ℓ	Semifocal length
c	$\omega\sqrt{\mu\epsilon}\ell$
u, v, ϕ	Three orthogonal coordinates
ξ	System of ellipses describing the u variation in the oblate and prolate spheroidal coordinate systems
η	System of hyperbolas describing the v variation in the oblate and prolate spheroidal coordinate systems
r, ϕ , θ	Spherical coordinate system coordinates
h_ϕ, h_u, h_v	Scale factors for the u, v, ϕ coordinate system
E_u, E_v, E_ϕ	Orthogonal components of the electric field intensity in the u, v, ϕ coordinate system
H_u, H_v, H_ϕ	Orthogonal components of the magnetic field intensity in the u, v, ϕ coordinate system
U(u)	Separable part of the field that varies with u
V(v)	Separable part of the field that varies with v
TM	Transverse magnetic (E_u, E_v, H_ϕ)
TE	Transverse electric (H_u, H_v, E_ϕ)
$Z_n^{(i)}(x)$	Spherical Bessel function of order n and type i
$h_n^{(2)}(x)$	Spherical Hankel function of the second kind of order n
$P_n^m(x)$	Legendre function of order n and degree m
$R_{ln}^{(i)}(c, \xi)$	Prolate spheroidal radial function of order n and type i
$S_{ln}(c, \eta)$	Prolate spheroidal angle function of order n
$R_{ln}^{(i)}(-ic, i\xi)$	Oblate spheroidal radial function of order n and type i
$S_{ln}(-ic, \eta)$	Oblate spheroidal angle function of order n
b	Semimajor axis dimension ($b = \ell\xi$)
a	Semiminor axis dimension ($a = \ell\sqrt{\xi^2 - 1}$)